

Singularity of Polystyrene Chains as the Hydrophobic Group of Amphiphilic Copolymers in Competitive Adsorption Processes: A Comparative Study of Polystyrene–Poly(ethylene oxide) and Poly(dimethyl siloxane)–Poly(ethylene oxide) Block Copolymers

Laurent Vonna, Hamidou Haidara,* and Jacques Schultz

Institut de Chimie des Surfaces et Interfaces, ICSI-CNRS, B.P. 2488, 15 Rue Jean Starcky, 68057 Mulhouse Cedex, France

Received August 4, 1999; Revised Manuscript Received February 8, 2000

ABSTRACT: Competitive adsorption kinetics of three diblock copolymers, a poly(dimethyl siloxane)–poly(ethylene oxide) and two polystyrene–poly(ethylene oxide), at a hydrophobic solid–oil–water interface are investigated, under a nonuniform distribution of the copolymer in the aqueous phase. When exposed to a variable concentration profile of the copolymer, the solid–oil–water interface evolves through a time-dependent shape reformation of the captive oil drop, which, for the two copolymers, reveals some strong qualitative differences. While the poly(dimethyl siloxane)–poly(ethylene oxide) adsorption results in a monotonically or stepwise shrinking of the captive drop in the whole range of the kinetics, the two polystyrene compounds exhibit a autophobic-like transition (early spreading/late stage shrinking). Based on the similarity in the number fraction of ethylene oxide units in the poly(dimethyl siloxane)–poly(ethylene oxide) and one of the polystyrene compounds, this adsorption induced wetting singularity is interpreted in terms of i) the competition between bulk retention and interface adsorption and, ii) the conformation and rearrangement barrier of the adsorbed segments, both driven by the polystyrene chain.

Introduction

Diblocks of polystyrene–poly(ethylene oxide) are among the most representative amphiphilic copolymers, both for their wide use in applications and the important literature dedicated to their fundamental investigations.^{1–10} This special and increasing interest is primarily driven by the variety of physicochemical properties exhibited by the two blocks of these molecules, which emerge in an equal richness of physical behavior of the PS-*b*-PEO, depending on the interacting environment (bulk, solvent, surface). Among these, one can mention (i) their basic interfacial activity in lowering the interfacial tension and compatibilizing two nonmiscible phases, (ii) their ability to stabilize through steric effects colloidal dispersions, and (iii) their self-organizing properties at mesoscopic length scale.⁸ For all these reasons and some of the singularities related to its adsorption,^{3,6,7} PS-*b*-PEO, either as neat material, in solution, or at interfaces, still remains attractive. As regards the bulk properties of PS-*b*-PEO diblocks in solution (micellization, diffusion coefficient, hydrodynamic radius) and their adsorption onto simple liquid–air, liquid–liquid, or solid–liquid interfaces, important results and data already exist from the above investigations.^{1–10} Still, these investigations often take place in homogeneous copolymer solutions, whereas the adsorption involves one single interface (oil–water or solid–water). The distinctive contribution and interest of the present work is that it addresses the competitive adsorption kinetics of these copolymers (PS-*b*-PEO versus PDMS-*b*-PEO) from a *nonuniform solution*, onto the *triple phase contact zone* (TPC) of a solid–oil–water (s–o–w) system. The *nonuniform* character here refers to the existence of a concentration profile of the copoly-

mer within the solution, which results, around the triple phase contact zone, in a time-dependent flux and competitive adsorption onto the interfaces (see below). Three diblock copolymers of low molecular weight (M_w) were used, a poly(dimethyl siloxane)–poly(ethylene oxide), PDMS-*b*-PEO (600–2400), and two polystyrene–poly(ethylene oxide)s, PS-*b*-PEO (1000–1000) and PS-*b*-PEO (1000–3000). The two numbers in the parentheses refer respectively to the molecular weight of the hydrophobic (PDMS and PS) and hydrophilic (PEO) side of the copolymers. These copolymers, especially the PS-*b*-PEO (1000–3000) and PDMS-*b*-PEO (600–2400), have similar number fraction $\phi = [n_{\text{DMS}}/(n_{\text{DMS}} + n_{\text{EO}})] \sim [n_{\text{S}}/(n_{\text{S}} + n_{\text{EO}})] \approx 0.13$, where n_{DMS} (=8) and n_{EO} (=55) represent the number of dimethyl siloxane and ethylene oxide units in PDMS-*b*-PEO and n_{S} (=10) and n_{EO} (=68) the number of styrene and ethylene oxide units in PS-*b*-PEO (1000–3000). The adsorption kinetics of these copolymers onto the (s–o–w) triple phase system is investigated under a nonuniform distribution of the copolymer in the surrounding water phase. The time evolution of this competitive adsorption is assessed from the shape reformation [radius $R(t)$ and contact angle $\theta(t)$] of the oil drop which is confined between the solid and the surrounding aqueous solution. Under these conditions, it is shown that the adsorption of the PDMS-*b*-PEO copolymer results in a monotonically or stepwise shrinking of the drop radius $R(t)$, whereas the two PS-*b*-PEO copolymers systematically evolve through an early stage spreading, followed by a late stage shrinking toward equilibrium. Related to this singularity, the final magnitude of reformation in the drop shape, $R(t_{\infty})$ and $\theta(t_{\infty})$, is significantly lower for the PS-*b*-PEO copolymers, as compared to those observed with PDMS-*b*-PEO or small nonionic alkyl poly(ethylene oxide) surfactants in earlier investigations.¹¹ The kinetics of these competitive adsorption and, especially, the sin-

* Corresponding author. E-mail address: H.Haidara@univ-mulhouse.fr.

gularity related to PS-*b*-PEO diblocks are discussed in this report, based on both energy and entropy considerations which mainly involve the PS and PDMS hydrophobic side chains.

Experimental Section

The two PS-*b*-PEO diblocks of general formula $(\text{CH}_2\text{-CHC}_6\text{H}_5)_n\text{-(OCH}_2\text{CH}_2)_m\text{OH}$ and respective molecular weights (1000–1000) and (1000–3000) for the PS and PEO blocks were from Goldschmidt AG. The index of polydispersity (M_w/M_n) for these copolymers was 1.12, as determined by gel permeation.¹² These amphiphilic copolymers have been extensively studied in bulk solutions, both by neutron, light scattering, surface tension, and fluorescence techniques, leading to an average critical micelle concentration (cmc) at the aqueous solution/air interface of $8.10 \approx 2.5 \times 10^{-5}$ g/mL ($\approx 6 \times 10^{-6}$ mol/L) for the PS-*b*-PEO (1000–3000) and $\approx 3.7 \times 10^{-6}$ mol/L for the PS-*b*-PEO (1000–1000). From the same investigations, a diffusion coefficient $D_0 \approx 10^{-11}$ m²/s at 25 °C and a hydrodynamic radius $R_h \approx 15$ nm were determined for diblock dilute solutions (0 to \sim cmc) of PS-*b*-PEO (1000–3000). The methyl-terminated PDMS-*b*-PEO copolymer of general formula $\text{CH}_3\text{[-OS(CH}_3)_2]_n\text{-(OCH}_2\text{CH}_2)_m\text{OH}$ has a dimethyl siloxane and ethylene oxide molecular weight of 600 and 2400, respectively, and was supplied by Polysciences, Inc., Eppelheim, Germany. The cmc of this surfactant-like copolymer as we determined by surface tension measurement at aqueous solution/air interface, using the Wilhelmy plate method, is $\sim 10^{-3}$ g/mL ($\sim 3.3 \times 10^{-4}$ mol/L). This value is about 2 orders higher than the limit of free monomer solubility of PS-*b*-PEO (1000–3000). Two structural numbers are used to characterize the intrinsic hydrophobic–hydrophilic balance of the two reference copolymers, PS-*b*-PEO (1000–3000) and PDMS-*b*-PEO (600–2400). These are (i) the number of dimethyl siloxane (DMS) and styrene (S) units in the hydrophobic chains, $n_{\text{DMS}} = 8$ and $n_{\text{S}} = 10$, and (ii) the number fractions $\phi_{\text{DMS}} = [n_{\text{DMS}}/(n_{\text{DMS}} + n_{\text{EO}})]$ and $\phi_{\text{S}} = [n_{\text{S}}/(n_{\text{S}} + n_{\text{EO}})]$, respectively, equal to ≈ 0.13 , for a number of ethylene oxide units n_{EO} in PS-PEO (1000–300) and PDMS-PEO equal to 68 and 55. Both copolymers were used as received, without any further purification. The oil phase used in these experiments, a squalane (C30) of 99% purity from Aldrich had a density $\rho = 0.810$, a viscosity $\eta = 21$ mPa·s, and a surface tension γ of 28.5 mN/m as measured by the Wilhelmy plate method. For both experiments, a deionized and doubly distilled freshwater of surface tension $\gamma = 72.3$ mN/m was used. The solid substrates were methyl-terminated hydrophobic molecular films of *n*-hexadecyltrichlorosilane, $\text{Cl}_3\text{Si(CH}_2\text{)}_{15}\text{CH}_3$ (referred to as HTS), self-assembled onto silicon wafers. The elaboration of these molecular films first involves the cleaning of the silicon wafers in a piranha solution ($\text{H}_2\text{O}_2/\text{H}_2\text{SO}_4$, 3/7 v/v), followed by a thorough rinsing with pure water. This pretreatment is aimed to develop a high silanol density at the silicon surface where the chlorosilane will self-assemble upon hydrolysis. The self-assembling is achieved by immersing for 12 h (at 20 °C) the clean silicon wafers into millimolar solutions of HTS in carbon tetrachloride. A detailed description of this surface modification has been presented elsewhere.¹¹ The surface energy of these model hydrophobic surfaces mainly exposing a methyl carpet was $\gamma_{\text{S}} = 21.5$ mN/m, and their dynamic contact angles at advancing and receding against water were respectively $\theta_{\text{A}} = 115^\circ$ and $\theta_{\text{R}} = 105^\circ$, at a velocity of the triple line $= 20$ $\mu\text{m/s}$.

Adsorption Kinetics. The experimental setup is shown in Figure 1 and is basically composed of a polystyrene working cell divided into three compartments of equal size which communicate through two holes. The substrate is first placed in the central compartment, and about 10 mL of freshwater is introduced in this cell. About 2 μL of squalane (C30) droplet is then deposited onto the substrate, leading to the formation of the virgin triple phase contact: the substrate/captive drop/surrounding water. The whole setup is allowed for about 30 min to equilibrate at the temperature of the experiments which is set at 22 °C. The resulting contact angle of the drop in this virgin system is $22^\circ \pm 2$ upon equilibration and remains stable

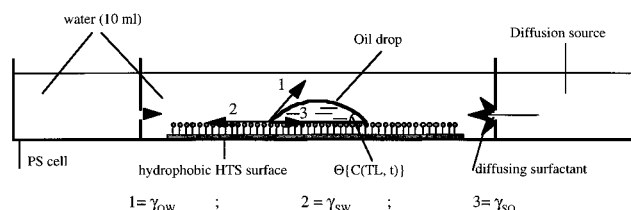


Figure 1. Schematic side view of the experimental setup. The central compartment is deliberately enlarged for details.

about this initial value at least over 10 h, as we verified in a reference experiment. The nonuniform distribution of the copolymer in the aqueous phase is produced by allowing the homogeneous copolymer solutions initially prepared in the lateral compartments to diffuse toward the central one containing the virgin system (solid–drop–pure water). Prior to this operation, the lateral compartments are disconnected from the central one by plugging the two holes with a paraffin film, and the homogeneous lateral compartments solutions (reservoirs = diffusion sources) are prepared by introducing a small amount (< 500 μL) of a fresh copolymer stock solution to give a diffusion source concentration C_{S} in each lateral reservoir. Upon equilibration of the whole system, the (s–o–w) interface and reservoir solutions, the holes are unplugged, allowing the reservoirs to diffuse toward the (s–o–w) triple phase contact, in the central compartment. This way, a symmetrical spatio-temporal concentration profile $C(r, t)$ is established with respect to the captive drop, leading to a time-dependent local flux $J(t)$ of copolymers around the triple phase contact zone (TPC), which in the low concentration approximation or in the early stage of the adsorption scales as $J(t, \text{TPC}) \sim -D[dC(r, t)/dt]$. A time-dependent adsorption then sets onto the interfaces, which kinetics are a function of the magnitude of the flux $J(t, \text{TPI})$. For the given experimental setup and system shown in Figure 1, this interfacial flux is essentially determined by the concentration of the diffusion sources (reservoirs), C_{S} , which in these experiments lies between 1.5 and 45 times the cmc *per reservoir*. The volume of water being identical in each compartment, the final equilibrium bulk concentration in the working cell at infinite time (C_{∞}) spans from ≈ 1 to ~ 30 times the cmc.

In the following, we will mainly refer to the physical parameters which completely characterize our experiments, the copolymer concentration in the reservoirs C_{S} , and related final bulk concentration (at equilibrium) in the working cell, C_{∞} . While the former governs the adsorption kinetics through the magnitude and time dependence of the local flux $J(\text{TPC}, t)$, the latter accounts for the maximum attainable magnitude of reconfiguration by the system at the thermodynamic equilibrium, both being related by a simple proportion.

The adsorption kinetics and related shape reconfiguration of the captive drop [$R(t)$, $\theta(t)$] were recorded using an automatic contact angle analyzer (Krüss G2), fitted with a video camera device. The drop radius is given in pixel units, the initial size ($t = 0$) being on average $2R(0) = 500$ pixels (~ 2.5 mm). Typical time intervals of data acquisition were 30 s, for the initial stage of the kinetics, and 1–5 min for the late stage. It is worth mentioning here that the polystyrene cell chosen for experimental convenience (realization of compartments and holes) has no noticeable incidence on the experimental results, at least for these copolymers and within the limit of concentrations used. This has been checked by using a glass cell under slightly different setup but for similar concentration profiles $C(r, t)$ and identical equilibrium bulk concentrations C_{∞} . Though less reproducible, these results were comparable in both the time evolution and magnitude of the drop shape reconfiguration to the optimized polystyrene cell setup. For all the experimental data presented in the following, the reproducibility of the results regarding the basic phenomenon under consideration (wetting inversion with PS-*b*-PEO versus monotonic shrinking of the drop with PDMS-*b*-PEO and their relative magnitude) has been verified over three series of experiments, for each diffusion source concentration C_{S} .

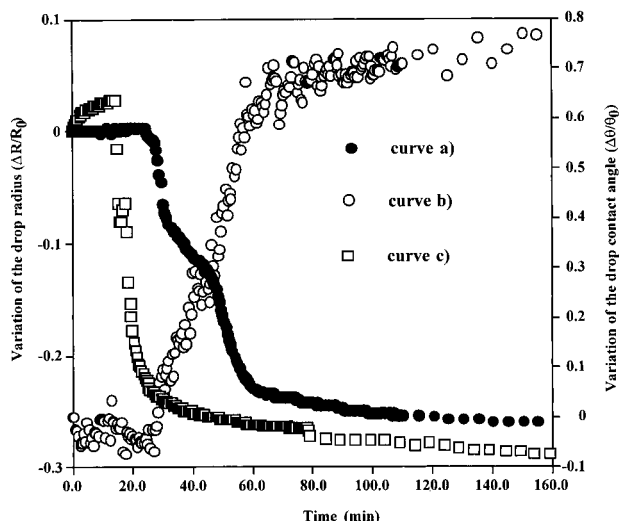


Figure 2. Adsorption kinetics of PDMS-*b*-PEO (600–2400) in normalized drop radius $R(t)$ and contact angle $\theta(t)$: (curve a) left-hand side ordinate ($\Delta R/R$), diffusion source concentration $C_S = 1.5$ cmc; (curve b) right-hand side ordinate ($\Delta\theta/\theta$), diffusion source concentration $C_S = 1.5$ cmc; (curve c) left-hand side ordinate ($\Delta R/R$), diffusion source concentration $C_S = 7.5 \times$ cmc.

Further, even under less well performed experimental conditions leading to less symmetrical shape reformation of the drop, this characteristic singularity is observed for the time evolution of PS-*b*-PEO, as compared to PDMS-*b*-PEO. On the other hand, the dispersion on these results, as expressed by the absolute value of the time-dependent drop parameter $R(t)$ for a given concentration profile (diffusion source concentration C_S), was $\varepsilon[R(t)] = \pm 10$ pixel units. This dispersion is reasonable for such dynamic experiment, since it involves both the dispersion on the initial value $\varepsilon[R(0)]$, the zero time lag, and intrinsic spacio-temporal fluctuations of the concentration profile within a series of experiments.

Results and Discussion

The adsorption kinetics for the PDMS-*b*-PEO onto the (s-C30-w) are given in Figure 2. The different curves represent the time evolution of the captive C30 drop parameters, $\Delta R(t)/R_0$ and $\Delta\theta(t)/\theta_0$, for a concentration of the diffusion source C_S per reservoir respectively equals 1.5 cmc (curve a and b in normalized radius and contact angle) and 7.5 times cmc (curve c in normalized radius). The equilibrium bulk concentration in the working cell, C_∞ , corresponding to these diffusion sources of 1.5 and 7.5 times the cmc are respectively $C_\infty = 1$ and 5 times the cmc. Except for the initial short transient spreading (< 2 min) observed in some of the experiments and which magnitude generally lies within the experimental dispersion, these adsorption kinetics are mainly characterized by a monotonically (or stepwise) shrinking of the confined drop radius toward the final equilibrium state. Because of the strong hydrophobic nature of the "HTS (methyl carpet)/C30" interface and the relative importance of the PEO group in these amphiphilic copolymers, their extraction from the aqueous phase (bulk water or s-w interface) and transfer (adsorption) to the (HTS/C30) interface will involve a much too high energy. One then can reasonably assume, for these systems, that none of these amphiphilic diblocks is brought to the (s-C30) interface which therefore remains free from adsorption, leading to zero time dependence of its interface tension, $d\gamma_{SO}(t) \equiv 0$. On the basis of this assumption, the shape reformation of the

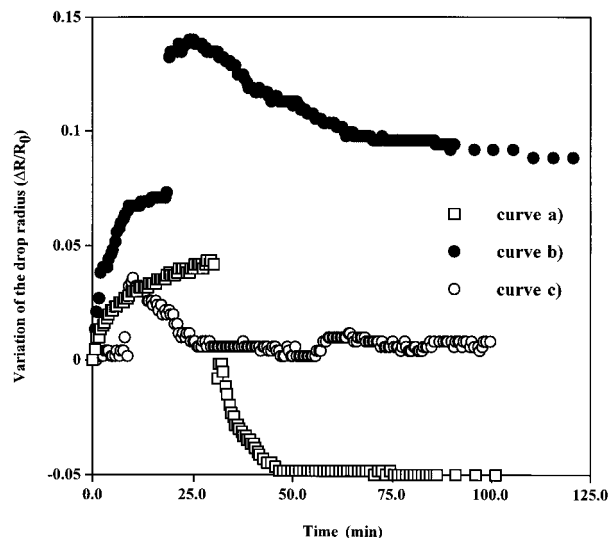


Figure 3. Adsorption kinetics of PS-*b*-PEO copolymers in normalized drop radius: (curve a) PS-*b*-PEO (1000–1000) at a diffusion source concentration $C_S = 4.5 \times$ cmc; (curve b) PS-*b*-PEO (1000–3000) at a diffusion source concentration $C_S = 22 \times$ cmc; (curve c) PS-*b*-PEO (1000–3000) at a diffusion source concentration $C_S = 45 \times$ cmc.

system during the adsorption is accounted for¹¹ by the time dependence of the Young equation

$$\gamma_{SW}(t) - \gamma_{SO}(0) = \gamma_{WO}(t) \cos \theta(t) \quad (1)$$

which time derivative gives

$$d\gamma_{SW}(t) - \cos \theta(t) d\gamma_{WO}(t) + [\sin \theta(t) d\theta] \gamma_{WO}(t) = 0 \quad (2)$$

Since the last term of eq 2 represents the contribution from the normal wetting force, the unique contribution from this time derivatives of the surface forces which drives the in-plane motion (spreading/shrinking) of the triple phase line (TPL) is therefore $d\gamma_{SW}(t) - \cos \theta(t) d\gamma_{WO}(t)$. For all our systems where $\theta(t)$ ranges from about 25° up to 70° , $\cos \theta(t)$ is a strictly positive quantity. Since the adsorption at both (s-w) and (o-w) interfaces results in an interfacial tension decrease ($d\gamma(t) < 0$), the condition for $[d\gamma_{SW}(t) - \cos \theta(t) d\gamma_{WO}(t)]$ to be ≤ 0 , leading to a monotonically or stepwise shrinking of the drop (Figure 2), finally amounts to $|d\gamma_{SW}(t)| \geq |d\gamma_{WO}(t)| \cos \theta(t)$. Therefore, the magnitude of the surface tension reduction at the (s-w) interface should predominate, during the kinetics, that of the in-plane component resulting from the (o-w) interface. This thermodynamic situation is simply expressed by a time-dependent unbalanced Young force, $F(t) = d\gamma_{SW}(t) - \cos \theta(t) d\gamma_{WO}(t)$, which for the PDMS-*b*-PEO diblock is < 0 , driving the retraction of the TPL (shrinking) as essentially observed in Figure 2.

The adsorption kinetics of the two PS-*b*-PEO diblocks, the (1000–1000) and (1000–3000), are shown in Figure 3. The curve a represents the PS-*b*-PEO(1000–1000), for a concentration of the diffusion source $C_S = 4.5$ times the cmc per reservoir and a final bulk equilibrium concentration in the working cell = 3 times the cmc. The curves b and c represent the PS-*b*-PEO (1000–3000) adsorption kinetics, for a reservoir concentration C_S respectively equal to 22 and 45 times the cmc. The bulk concentrations in the working cell at equilibrium, C_∞ , corresponding to these diffusion sources are respec-

tively 15 and 30 times the cmc. As it appears in Figure 3, the adsorption kinetics of these PS-*b*-PEO copolymers are characterized, as compared to the PDMS-*b*-PEO (Figure 2), by a singularity which clearly shows up in a wetting inversion (early stage spreading/late stage shrinking). Interestingly, this wetting inversion, as well as the characteristic time involved in the early stage spreading which is on the order of 25 min, are both independent of the concentration C_S of the diffusion source and molecular weight, (1000–1000) or (1000–3000), of PS-*b*-PEO copolymers. Related to the wetting singularity induced by the adsorption of the PS-*b*-PEO copolymers, a much lower magnitude in the shape reformation of the captive drop is observed in both spreading and shrinking modes, as compared to the PDMS-*b*-PEO diblock. For instance, at a diffusion source concentration C_S (in unit cmc) equals to 45 (Figure 3, curve c), a magnitude $|\Delta R(t)/R_0| < 0.05$ is observed on the equilibrium plateau for PS-*b*-PEO (1000–3000), against 0.25 for PDMS-*b*-PEO at $C_S = 1.5$ cmc (Figure 2, curve a). Because both PS-*b*-PEO (1000–3000) and PDMS-*b*-PEO (600–2400) have quite an identical hydrophilic/hydrophobic balance as estimated above by their number fractions $\phi_{\text{DMS}} \approx \phi_S \approx 0.13$, for $n_S \sim n_{\text{DMS}}$ and comparable n_{EO} , the qualitative difference exhibited by these copolymers may then arise from some specific behavior of the hydrophobic PS and PDMS groups during the competitive adsorption kinetics. If one starts from the aforementioned time-dependent driving force for the shape reformation of the captive drop, the initial spreading stage observed with PS-*b*-PEO then reads $F(t) = d\gamma_{\text{SW}}(t) - \cos \theta(t) d\gamma_{\text{WO}}(t) > 0$, which implies that $|d\gamma_{\text{SW}}(t)| > |d\gamma_{\text{WO}}(t)| \cos \theta(t)$, $d\gamma$ being < 0 in both cases. In term of the competition between the interfaces, this means that the incorporation kinetics of the PS-*b*-PEO (adsorbed amount Γ /unit time) at the (o-*w*) interface predominates, leading thereby to a stronger reduction in $\gamma_{\text{WO}}(t)$, as compared to $\gamma_{\text{SW}}(t)$ at the (s-*w*) interface. The overall picture of this competition in the initial stage is the spreading of the captive drop. Intuitively, one also could expect a strong adsorption of the PS-*b*-PEO at the (s-*w*) interface because of the hydrophobic PS group, which higher interfacial tension against water could drive a lower retention in the bulk aqueous phase, as compared to DMS chains ($\gamma_{\text{DMS-W}} \approx 39.5$ mN/m). The low (s-*w*) interface adsorption of PS-*b*-PEO in this initial stage, given at first approximation by the Gibbs relation, $\Gamma(t) \sim (-RT)^{-1} d\gamma_{\text{SW}}(t)[C(t)/dC(t)]$, can reasonably be accounted for by the high energy barrier associated with the PS-*b*-PEO incorporation at the (s-*w*) interface, $\Delta F = \Delta U - T\Delta S$. This free energy should be low enough to overcome the bulk retention of the copolymer, even in a relatively poor solvent of the hydrophobic tail as is water for PS. Assuming the variation in the interaction energy ΔU to be roughly comparable for both PS-*b*-PEO (1000–3000) and PDMS-*b*-PEO upon adsorption, the leading term in the above barrier is the configurational (entropy) constraint resulting from the confinement of the PS chains at the (s-*w*) interface. Though any adsorption process is accompanied with this entropy penalty ($-T\Delta S > 0$), the magnitude of this barrier is strongly dependent on the nature and structural (conformational) flexibility (rigidity) of the molecule. As compared to the highly flexible DMS chains,¹³ the intrinsic structural rigidity of the PS chains,¹³ mainly due to the phenyl rings, will contribute to increase both the height of the barrier ($-T\Delta S$) and

the characteristic relaxation time of interfacial rearrangement of the adsorbed chains. Very roughly, the bulk configuration entropy S_B can be related to the molecular volume $\Omega_B \sim (R_G)^3$ as $S_B \sim 3k(\ln R_G)$, where R_G is the radius of gyration of the chain and k the Boltzmann's constant. The entropy in the adsorbed state can be related in a similar way to the area $\omega_A = \pi(R_G)^2$ as $S_A \sim 2k(\ln R_G)$ for molecules such as PDMS chains which can explore by segmental flexibility the whole interfacial area (configurations)

$$\omega_A = \int_0^{R_G} R dR \int_0^{2\pi} d\varphi$$

For PDMS-*b*-PEO, the corresponding entropy penalty is simply given by $(S_A - S_B) \sim k \ln(1/R_G)$. For the less flexible PS chains adsorbed at the (s-*w*) interface, the "areal" configuration is reduced from $\omega_A \sim \pi(R_G)^2$ to about

$$\omega_A^* \sim \int_{\delta>0}^{R_G} R dR \int_0^{2\pi} d\varphi = \pi(R_G^2 - \delta^2)$$

the configurational occupancy along the dimension extending from $R \gtrsim 0$ (maximum folded chain) to $R = R_G$ (fully stretched chain), being restricted to some corona of width $(R_G - \delta)$. The corresponding entropy variation is much higher, as compared to PDMS chains,

$$(S_A - S_B) \sim k \ln[(R_G^2 - \delta^2)/R_G^3]$$

the difference being on the order of $\ln(1 - \delta^2/R_G^2)$ and arising in a higher PS adsorption barrier ΔF through ($-T\Delta S$). Within this picture of less conformational flexibility of the PS chains against PDMS,¹³ the entropy and conformation limited adsorption appears to be the driving mechanism for the spreading of the captive drop observed in the early stage of the adsorption kinetics of PS-*b*-PEO copolymers. Along with this wetting inversion related to the above specific features of the PS chain as the hydrophobic side of these PS-*b*-PEO copolymers, one can interestingly mention the influence of the diffusion source concentration C_S as this appears through relative magnitude of the drop shape reformation, at different C_S (Figure 3). Though not systematically investigated over a sufficiently wide range of concentrations, a clear decrease in both the magnitude $|\Delta R(t)/R_0|$ and characteristic time scale involved in the wetting inversion were observed in a fairly reproducible way, at high diffusion source concentration (Figure 3, curves a and c). In fact, such a dependence is physically relevant, since an increase in C_S would result at the triple phase line in a higher flux $J(\text{TPL}, t = 0)$, in the early time of the kinetic. As a consequence, the higher subsurface concentration $C(\text{TPL}, t = 0)$ and chemical potential difference $\Delta\mu_{\text{SW}}$ established at the (s-*w*) interface will drive an adsorption amount Γ_{SW} , which is enough important to significantly lower the interfacial tension through $d\gamma_{\text{SW}}(t = 0) \sim -RT\Gamma_{\text{SW}}[dC/C]_{t=0}$. Along with that lowering in γ_{SW} , both the time scale and magnitude of the initial spreading force on the captive drop are significantly reduced, leading to the observed modification in the Young force balance, as discussed above, from eqs 1 and 2.

Conclusion

We have investigated the competitive adsorption kinetics of two standard low molecular weight diblock

copolymers, PS-*b*-PEO and PDMS-*b*-PEO, from strongly nonuniform solutions, onto the triple phase interface of a (solid–oil–water) system. Simple experimental setup and surface thermodynamics are used and shown to be as efficient and powerful as most of light scattering techniques in revealing subtle molecular events at interfaces. These investigations revealed some unexpected singularities in the adsorption kinetics of PS-*b*-PEO copolymers against PDMS-*b*-PEO which were analyzed, based on the configurational entropy penalty associated with the lesser structural flexibility of the PS side chain in PS-*b*-PEO copolymers.

References and Notes

- (1) Kanellopoulos, A. G.; Owen, M. J. *J. Colloid Interface Sci.* **1971**, *35*, 120–125.
- (2) d'Oliveira, J. M. R.; Xu, R.; Jensma, T.; Winnik, M. A.; Hruska, Z.; Hurtrez, G.; Riess, G.; Martinho, J. M. G.; Croucher, M. D. *Langmuir* **1993**, *9*, 1092–1097.
- (3) Cosgrove, T.; Zarbakhsh, A.; Luckam, P. F.; Hair, M. L.; Webster, J. R. P. W. *Faraday Discuss.* **1994**, *98*, 189–201.
- (4) Budkowski, A.; Klein, J.; Fetters, L. J.; Hashimoto, T. *Macromolecules* **1995**, *28*, 8579–8586.
- (5) Fytas, G.; Anastasiadis, S. H.; Seghrouchni, R.; Vlassopoulos, D.; Li, J.; Factor, B. D.; Theobald, W.; Toprakcioglu, C. *Science* **1996**, *274*, 2041–2043.
- (6) Tripp, C. P.; Hair, M. L. *Langmuir* **1996**, *12*, 3952–3956.
- (7) Pagac, E. S.; Prieve, D. C.; Solomentsev, Y.; Tilton, R. D. *Langmuir* **1997**, *13*, 2993–3001.
- (8) Mortensen, K.; Brown, W.; Almdal, K.; Alami, E.; Jada, A. *Langmuir* **1997**, *13*, 3635–3645.
- (9) Gonçalves da Silva, A. M.; Simoes Gamboa, A. L.; Martinho, J. M. G. *Langmuir* **1998**, *14*, 5327–5330.
- (10) Jada, A.; Hoffstetter, J.; Siffert, B. In *Short and Long Chains at Interfaces, Proceedings of the XXXth Reeencontres de Morion*; Morion Condensed Matter Physics Series; Daillant, J., Guenoun, P., Marques, C., Muller, P., Tràn, T. V. J., Eds.; Frontières: Gif-sur-Yvette, France, 1995; p 41.
- (11) Haidara, H.; Vonna, L.; Schultz, J. *Langmuir* **1996**, *12*, 3351–3355.
- (12) Berger, M.; Richtering, W.; Mülhaupt, R. *Polym. Bull. (Berlin)* **1994**, *33*, 521.
- (13) Brandrup, J.; Immergut, E. H.; In *Polymer Handbook*, 2nd ed.; Brandrup, J., Immergut, E. H., Eds.; Wiley-Interscience: New York, 1975; p IV-48.

MA991299C